2

Deep structure of peninsular Italy from seismic tomography and subcrustal seismicity

GIOVANNI BATTISTA CIMINI and ALESSANDRO MARCHETTI

Istituto Nazionale di Geofisica e Vulcanologia, Roma, Italy

The upper mantle structure beneath penisular Italy is investigated through tomographic reconstruction of the *P*-wave velocity field down to 600 km and spatial distribution of subcrustal earthquakes. The tomographic images are computed using a non-linear technique to invert an improved dataset of teleseismic arrival times recorded by the Italian National seismic network in the last fifteen years. For the deep seismicity analysis, we selected 445 events from the database of subcrustal earthquakes that occurred in the period 1988-2004 (1191 events). A subset of 30 earthquakes including most of the deepest foci were relocated using the Hypoellipse location program and an upper mantle velocity structure based on the spherical ak135 global model. The velocity maps show a remarkable complexity of the lithosphere-asthenosphere system of the region, depicting different styles of lithospheric sinking along peninsular Italy from the Northern Apennines to the Calabrian Arc. The subducting slabs include most of the upper mantle events, but only in part they are seismically active.

2.1. Introduction

The present-day tectonic setting of the Italian Peninsula is the result of a complex collision process between the African and Eurasian plates, active since at least 65 Myr (Dercourt *et al.*, 1986; Dewey *et al.*, 1989; Patacca *et al.*, 1990). According to one of the most accepted geodynamic models, the evolution of this part of the Central Mediterranean area after the Alpine orogenesis was driven by the eastward migration of the Adriatic-Ionian lithosphere through a complex subduction system (Malinverno and Ryan, 1986; Faccenna *et al.*, 1996; Gueguen *et al.*, 1998). The numerous tomographic studies developed in the last two decades have contributed to constrain the past tectonic processes mapping the three-dimensional (3D) heterogeneous velocity structure of the crust and upper mantle beneath the region. From these investigations, characterized by the use of different arrival times datasets, inversion techniques, and parameterization of the Earth's interior within the target volume, strong, broad high-velocity bodies have been reconstructed in the lithosphere-asthenosphere system of the Apennines and surrounding seas.

In regions of plate boundaries, deep tectonic processes, such as lithospheric subduction, continental collision, and magmatism generate strong thermal heterogeneities, the primary cause of anomalies in the propagation of seismic waves. Following the wide literature on seismic tomography, the existence of High Velocity Anomalies (HVA) in the upper mantle is generally interpreted as due to cold (dense) oceanic lithosphere which penetrates into a warm (soft) asthenosphere characterized by lower velocity (Hirahara and Hasemi, 1993; Lay, 1994). A more critical point is inferring from tomographic reconstructions the type of lithosphere involved in the subduction process. Below the Tyrrhenian-Apennines region, the presence of subducted lithosphere of both oceanic and continental-

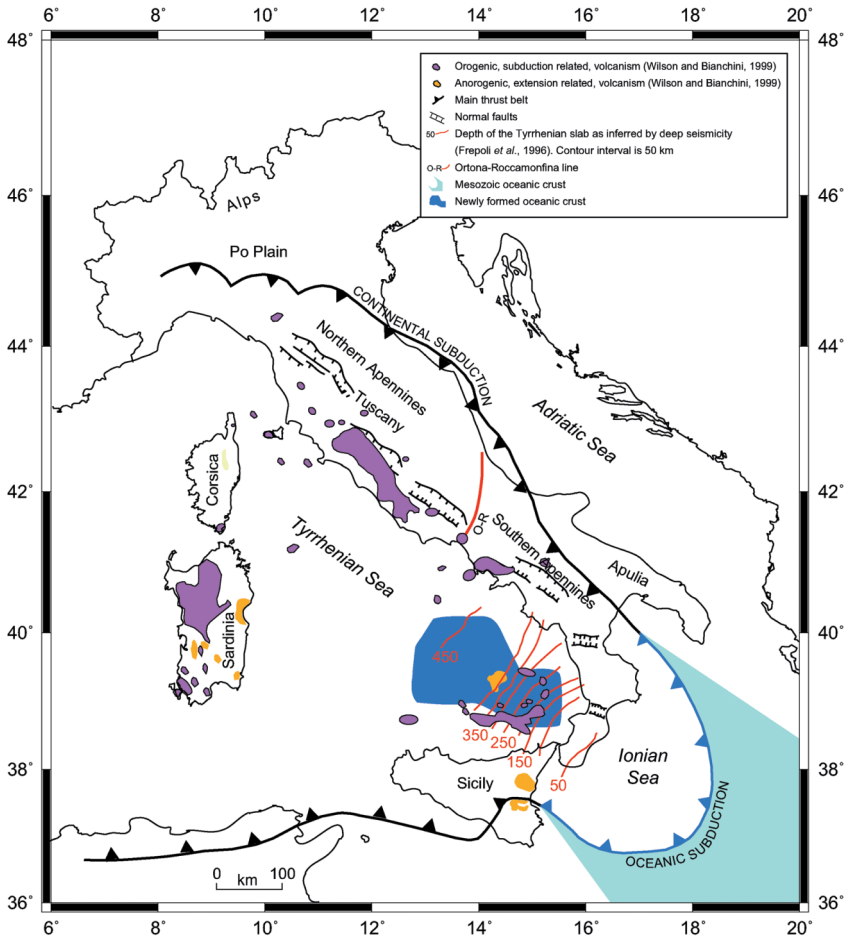

Fig. 2.1. Map of the Italian region showing the main seismotectonic features. Continental and oceanic subductions are expected to occur in the Northern Apennines and Calabria-Southern Tyrrhenian Sea, respectively. Beneath the Central-Southern Apennines the situation is more complex, probably reflecting the transition between the two different types of lithospheric sinking.

type has been hypothesized as a result of the collision process (Carminati *et al.*, 2002; fig. 2.1). Indeed, when the subduction zone reaches the continental lithosphere, the latter may be pulled down by the sinking oceanic lithosphere. The existence of lithospheric slabs in the upper mantle (either oceanic or continental) is supposed to cause higher velocities with respect to the surrounding asthenosphere, that can be recovered by seismic tomography if a thermal contrast is mantained.

In this study, after reviewing the main features of the deep structure of the region obtained by previous tomographic analysis, we show results from a new three-dimensional *P*-wave velocity model, enhancing the along-strike complexity of the Apenninic subduction system. Then we focus on the spatial distribution of subcrustal earthquakes as independent constraint on the geometry and rheology of the lithospheric sinking inferred from tomography.

2.2. Upper mantle tomography studies: a review

The study of the upper mantle structure using arrival times seismic tomography started in Italy in the early 1980s after the first reliable inversion technique was devoloped (Aki *et al.*, 1977). The first three-dimensional *P*-wave velocity model of Italy was produced by Scarpa (1982) inverting teleseismic *P* and *PKP* data taken from bulletins. The model revealed marked velocity contrasts especially in the deep structure of the Southern Tyrrhenian Sea, although with no satisfying resolution. Further attempts with teleseisms were those of Babuska and Plomerová (1990), that evidenced high velocities beneath the Alps and the Northern Apennines, but still suffered from the use of poor quality data. The travel-time tomography by Spakman *et al.* (1993) investigates the European-Mediterranean mantle structure down to 1400 km, by inverting a huge dataset of arrival times ($\sim 10^6$) of both regional and teleseismic events. This study, based on *P* delay time data collected by the International Seismological Centre (ISC) in 18 years of observation, represents a considerable extension of earlier tomographic experiments. In the same period, Amato *et al.* (1993) and Cimini and Amato (1993) computed different *P*-wave velocity models of Italy and surrounding seas using smaller datasets ($\sim 10^3$) characterized by high precision in the estimate of phase arrival times and by a more homogeneous azimuthal coverage of the ray sampling. Compared to the use of noisy bulletin data, the use of accurately picked arrival times significantly improves the fit of the data, and the spatial resolution of the tomographic images. Both these approaches, apart from differences in the reconstruction of the velocity contrasts and in the geometry of lateral heterogeneities, found consistent high-velocity anomalies below peninsular Italy which were interpreted as remnants of subducted lithospheric slabs underlying the region.

More recent investigations of the deep structure of Italy are those by Cimini and De Gori (1997), Piromallo and Morelli (1997, 2003), Lucente *et al.* (1999), Di Stefano *et al.* (1999). In the study by Cimini and De Gori (1997), both direct (*P* and *PKPdf*) and secondary (*pP*, *sP*, *PcP*) *P*-wave arrival times were used to improve the sampling of the target volume and to reduce smearing effects. The tomographic model obtained by Lucente *et al.* (1999) extends the definition of the deep structures beneath both the Alps and the Apennines down to 800 km depth. The main finding is a nearly continuous pattern of high-velocity anomalies located between 250 and 670 km depth below the Apennines, shifting toward the Tyrrhenian Basin with increasing depth. The paper by Di Stefano *et al.* (1999) focuses on the *P*-wave velocity structure in the crust and uppermost mantle of Italy. They used a large dataset of arrival times of crustal earthquakes to retrieve the lateral heterogeneities at three depth levels located in the upper crust, lower crust, and beneath the Moho. The tomographic image for the lower crust (layer 2, 22 km depth) shows a pronounced low-velocity belt beneath the entire Apennines. This feature was interpreted by the authors as an effect of high temperatures caused by upwelling of asthenospheric material in front of the Adriatic slab. Finally, the *P*-wave tomography carried out by Piromallo and Morelli (2003) is an improved picture of the distribution of large-scale fast anomalies in the mantle of the Euro-Mediterranean area down to 1000 km depth. The pattern revealed by their 3D velocity model for the area under study suggests a mantle dynamics dominated by blockage of subducted slabs at the upper mantle-lower mantle boundary and accumulation of recumbent fast material within the transition zone. This result corroborates the horizontal deflection of the Southern Tyrrhenian slab previously imaged by Cimini (1999).

2.3. The *P*-wave velocity structure down to 600 km

Most of the tomographic studies quoted in the previous section were carried out by using a linear approach to solve the non-linear inverse problem relating the travel time residuals to the unknown velocity anomalies. The linearization of the tomographic problem, which neglects the seismic rays' bending induced by the 3D velocity heterogeneities, may become highly inadequate when trying to

image Earth volumes with strong velocity contrasts, such as high-velocity lithospheric slabs or low-velocity asthenospheric zones, magma chambers, etc.

In this study, to further improve the velocity model of the study region we use a non-linear teleseismic tomography technique that incorporates a robust minimum travel time ray tracing for accurate ray paths and travel times computation in 3D media. The method, previously applied to the deep structure of Southern Italy by Cimini (1999) and Cimini and De Gori (2001), performs an iterative inversion scheme that repeatedly computes a damped least square solution of the linearized problem and recalculates the ray trajectories through forward modelling. By iterating, the velocity field is reconstructed gradually and larger data misfit reduction are usually achieved with respect to single step inversion (Cimini and De Gori, 2001).

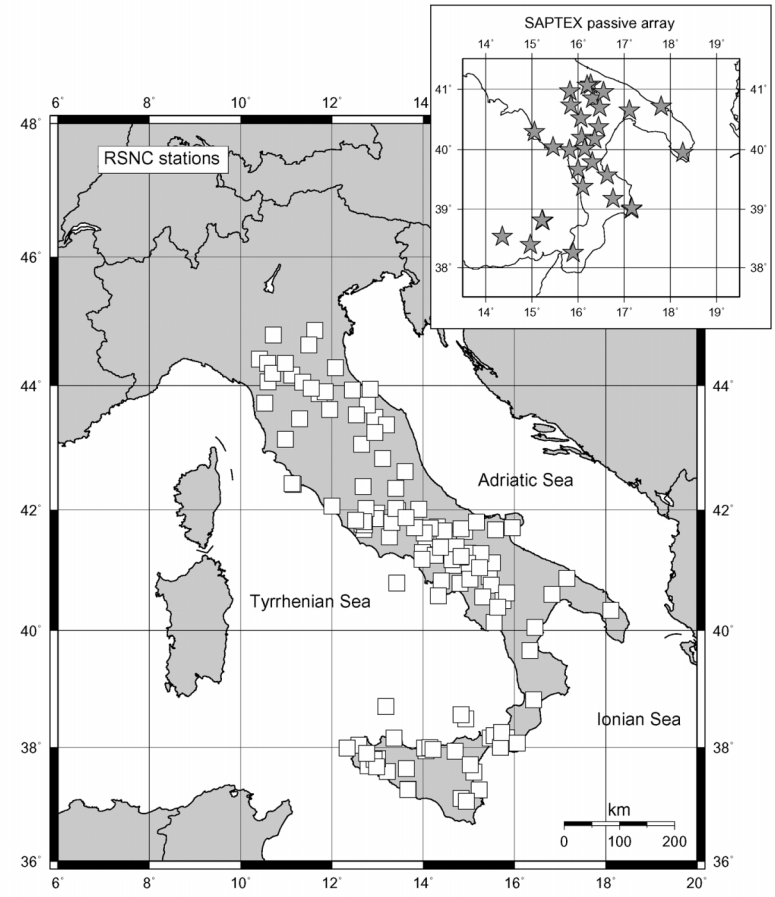

Fig. 2.2. Location of the permanent stations of the Istituto Nazionale di Geofisica e Vulcanologia (INGV) seismic network used in this study (white squares). In the panel, grey stars indicate the recording sites occupied by the three-component stations of the SAPTEX passive array during the period 2001-2004. Data recorded by these stations have contributed significantly in improving the relocation of subcrustal earthquakes in Southern Italy.

The data we used for the tomography consists of 120 teleseisms selected from over 500 $M_w \geq 5.5$ distant earthquakes ($\Delta > 30°$) recorded by the stations of the Italian National seismic network (RSNC) in the past fifteen years (fig. 2.2). To this dataset we added some hundreds of high-quality teleseismic waveforms produced by the SAPTEX temporary array (Cimini *et al.*, 2006) deployed in Southern Italy during 2001-2004 (see panel in fig. 2.2). We retained events with at least 30 *P*-wave arrival times. Moreover, to obtain a more homogenous sampling of the target volume, we set an upper boundary value to the number of allowable ray trajectories coming from back azimuth-epicentral distance sectors of 15°×15°. The sources giving additional paths were ignored. This equalization attempts to reduce the contribution of the oversampled approaching directions (*e.g.*, backazimuths in the NE quadrant for our region), thus limiting spurious mapping of velocity anomalies given by smearing along the predominant direction of illumination.

From the collected seismograms we estimated the arrival times of 5585 *P* phases (4425 *P*, 244 *Pdiff*, and 916 *PKPdf*). The iterative inversion was performed by parameterizing the deep structure beneath peninsular Italy and adjacent seas with a three dimensional grid of nodes whose parameters are listed in table 2.I. The centre of the grid (x=0, y=0) corresponds to the geographic coordinates 41.0N, 14.0E; the bottom layer (not inverted) was set at 700 km depth. We used the 1D velocity model ak135 (Kennett *et al.*, 1995) as background Earth's structure to compute theoretical *P*-wave arrival times and travel time residuals at the first iteration.

We carried out our non-linear tomography through five consecutive iterations. Most of the final variance improvement (+74.7%) was obtained after three iterations (+74.1%), starting from an initial data variance of 0.77 s^2, and no significant model changes were further achieved with the subsequent iterations. Figure 2.3 shows the trade-off curve between resolution and standard errors used to select the optimal damping parameter for the iterative inversion. We selected a damping value of 500 s^2 to have good average resolution (>0.5) and limited model standard errors (<1.0%).

Figure 2.4a-d shows four vertical slices through the 3D model with the *P*-wave velocity anomalies computed at the third iteration. These maps depict the different tectonic settings along peninsular Italy from the Northern Apennines to the Calabrian Arc. Section AA′ (fig. 2.4a) crosses the North-

Table 2.I. Parameters of the 3D grid model and starting *P*-wave velocities adopted for the iterative inversion.

Layer	Depth km	Nodes in x	Nodes in y	Δx km	Δy km	Vp km/s
0	0	Station layer-151 recording sites				5.80
1	30	19	21	50	50	6.05
2	70	19	21	55	55	8.04
3	120	19	21	60	60	8.05
4	180	19	21	65	65	8.22
5	250	19	21	70	70	8.45
6	350	19	21	80	80	8.81
7	450	19	21	90	90	9.49
8	600	19	21	100	100	10.00
9	700	19	21	110	110	10.90

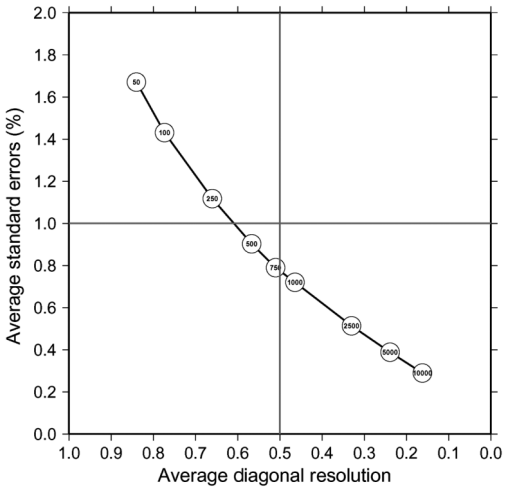

Fig. 2.3. Trade-off curve between average diagonal resolution and average standard error computed for selecting the optimal damping parameter of the iterative inversion.

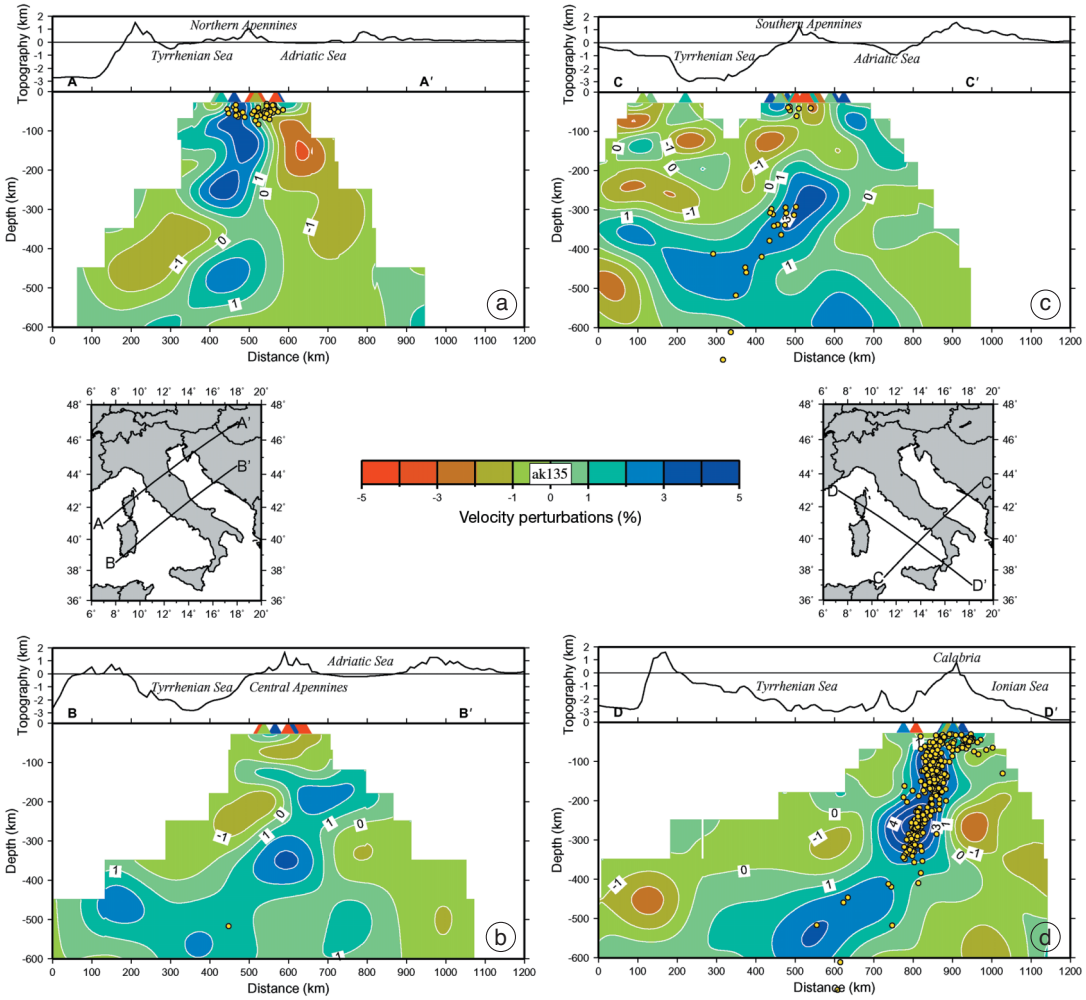

Fig. 2.4a-d. Cross sections through the 3D velocity model showing the geometry of the subducted lithosphere and its relationship with the surrounding mantle. Yellow circles depict earthquake hypocenters located within ±100 km from the vertical plane (bulletin localization). a) Beneath the Northern Apennines a continuous high-velocity body characterized by positive perturbations as large as +4% is imaged down to 300 km depth. The subcrustal seismicity is concentrated in the upper 100 km and it is only partially coincident with the fast structure. b) Beneath the Central Apennines the velocity pattern delineates a downgoing slab from ~100 km down to the bottom of the model. The slab is overlain by low-velocity regions extending from the uppermost mantle down to about 300 km below the Central Tyrrhenian Basin. No upper mantle events are observed within this segment of the Apenninic Range. c) Beneath the Southern Apennines the tomogram reveals a main, southwestward dipping high-velocity slab below about 200 km. This body appears detached from the shallower high-velocity anomaly below the Apulian foreland. Like the seismic structure, also the distribution of subcrustal earthquakes seems interrupt, suggesting the existence of two distinct seismogenic zones. d) This image shows the subduction of the Ionian oceanic lithosphere in the Southern Tyrrhenian area, along a NW-SE profile. The deep velocity structure is dominated by a strong high-velocity anomaly from the uppermost mantle down to ~350 km depth. Below this depth, a clear deflection of the deeper HVA to a nearly horizontal posture is observed. The pattern of shallow hypocentres (30<depth<70 km) delineates the bending of the subducting lithosphere beneath Calabria.

ern Apennines from the Tyrrhenian Sea to Dinarides. Below the belt, the teleseismic image reveals a strong (ΔVp=+4%), continuous HVA that extends from the base of the crust (~30 km) to about 300 km depth. A weaker HVA is reconstructed in the depth range 400-600 km, within the upper mantle transition zone. The tomogram suggests a ~100 km thick lithospheric slab steeply dipping toward the back-arc region (Tuscany) and in the Northern Tyrrhenian Basin at greater depths. Section BB′ (fig. 2.4b) is from the Tyrrhenian Sea, through the Central Apennines, to Dinarides. Here the velocity pattern shows a southwestward dipping HVA from about 100 km depth to the bottom of the present model. At uppermost mantle depths, the slab seems prolongated below the Adriatic Sea outside the sampled region. Section CC′ (fig. 2.4c) displays the complex seismic structure characterizing the Southern Tyrrhenian Sea and Southern Apennines. The main feature is a continuous high-velocity anomaly (ΔVp·+2÷+4%) reconstructed from about 200 km to 500 km depth. This body appears detached from the uppermost mantle HVA imaged beneath the Adriatic foreland. As in the previous SW-NE oriented slice, the geometry of the deeper portion of the fast structure indicates a subducting lithosphere that deflects horizontally within the transition zone beneath the Tyrrhenian Sea. Finally, section DD′ (fig. 2.4d) shows the upper mantle structure beneath the Southern Tyrrhenian Sea and Calabria along a NW-SE profile. The high-velocity body depicting the subducting slab, steeply dipping from the Calabrian Arc to the northwest, is observed from the uppermost mantle down to ~350 km. It includes all the intermediate and deep seismicity, which in the present study represents a completely indipendent dataset for recostructing the geometry of the subduction zone. Below ~400 km, the tomogram displays a subhorizontal HVA, possibly detached from the highly seismic upper portion. This deep HVA may represent the oldest portion of the subducted lithosphere which is presently stagnant in the transition zone (Cimini, 1999; Lucente *et al.*, 1999).

2.4. Upper mantle seismicity

In addition to seismic tomography, another important contribution to the delineation of the deep structure in regions of plate boundary comes from the distribution of intermediate and deep earthquakes foci. In peninsular Italy, subcrustal earthquakes are observed below the Northern Apennines and the Calabrian Arc. The paucity of seismicity in the upper mantle beneath the Central-Southern Apennines, along with the lack of clear high-velocity anomalies inferred from tomography, led various authors to suggest that the subduction has not been continuous beneath the whole Apenninic Arc.

Figure 2.5 shows the spatial distribution of 445 subcrustal events extracted from the INGV bulletin 1988-2004. This database consists of about 1200 earthquakes that we have selected by looking at the number of recording phases (NPH≥15), the horizontal and vertical errors (ERH≤10 km, ERZ≤15 km), and the final root-mean-square travel time residual (RMS≤1.0 s). In the Northern Apennines the pattern displays a ~350 km long uppermost mantle seismogenic zone located beneath the axis of the chain. The seismicity follows the bend of the Northern Apenninic Arc and is apparently concentrated in two adjacent NW-SE trending zones as previously observed by Selvaggi and Amato (1992). In Southern Italy, most of subcrustal earthquakes occur below the Southern Tyrrhenian area adjacent to Calabria. The deep seismicity extends laterally for about 300 km and is mostly concentrated in depth range 70÷300 km (intermediate foci). The subcrustal earthquakes located beneath the Ionian Sea and the Calabrian Arc depict a subhorizontal seismic zone probably related to the upper portion of the subduction zone delineated by seismic tomography (Selvaggi and Chiarabba, 1995; Frepoli *et al.*, 1996; Cimini, 1999; this work). Below ~300 km depth the distribution appears to be shifted northwestward in the Central Tyrrhenian Basin (blue circles in fig. 2.5), according to the lateral deflection of the subducted lithosphere within the transition zone observed in fig. 2.4d, cross-section DD′, and by Cimini (1999).

The main purpose of this analysis is to provide a better picture of the spatial distribution of subcrustal earthquakes with respect to the upper mantle seismic structure derived from tomography. To

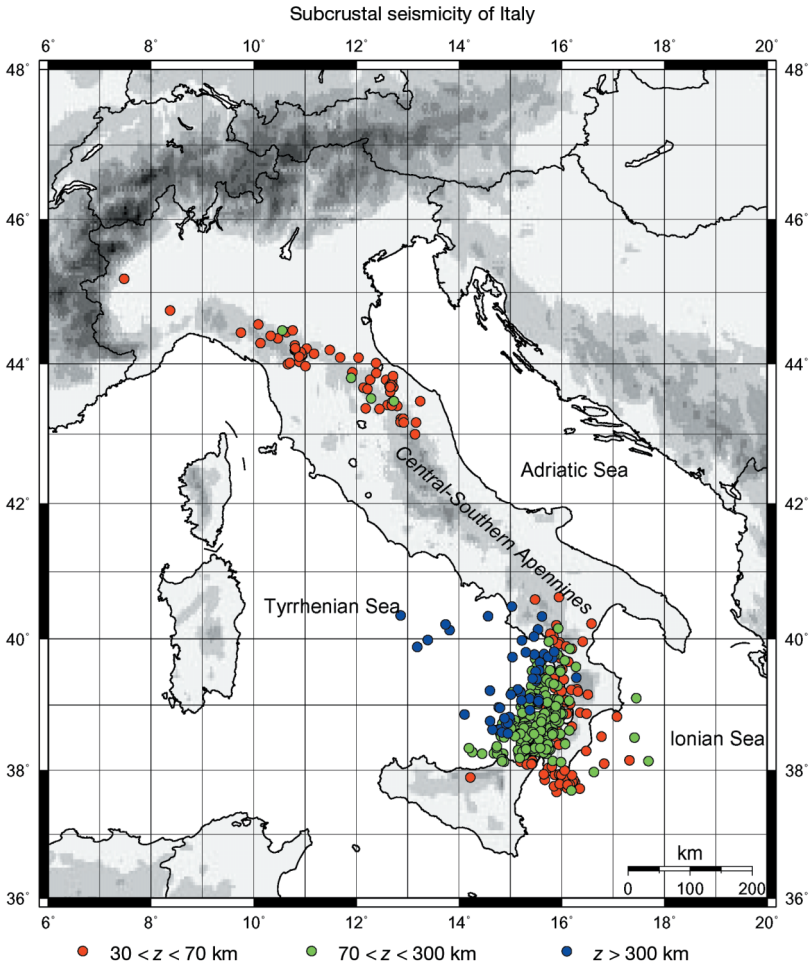

Fig. 2.5. Subcrustal seismicity selected from the INGV dataset in the period 1988-2004: red circles are the shallow foci (30<z<70 km); green circles are the intermediate foci (70<z<300 km); blue circles are the deep foci (z>300 km). Note the absence of subcrustal seismicity in the Central-Southern Apennines between approximately 41°N and 43°N, and the northwestward migration of the deep seismicity (h>300 km) of the Southern Tyrrhenian subduction zone.

achieve this goal we re-picked the *P*/*S* arrival times and re-examined the hypocentral location of 30 subcrustal events extracted from the dataset displayed in fig. 2.5. This subset includes all the intermediate foci observed in the Northern Apennines region (green circles in fig. 2.5) and most of the deep earthquakes located in the transition zone (410<z<660 km) and lower mantle beneath the Southern Tyrrhenian Sea. Improving the location of the deepest events is particularly important for constraining the depth extension of the seismogenic slabs. We also relocated many of the subcrustal events that occurred in the Southern Apennines and Basilicata, in order to confirm their upper mantle origin within the complex seismic structure caused by the transition from the oceanic subduction

beneath Calabria and Southern Tyrrhenian Sea to the continental collision/subduction in the region (see fig. 2.4c). The original locations obtained by INGV using a HYPO71-based code and a Earth's velocity model built up of two crustal layers ($z1$=10 km, Vp=5.0 km/s; $z2$=20 km, Vp=6.0 km/s) over a half space (Vp=8.20 km/s) are listed in table 2.II. The hypocentral parameters computed using the Hypoellipse program (Lahr, 1999) with the ak135 1D velocity model are given in table 2.III. For the relocation of the subcrustal events which have occurred in Southern Italy since July 2001 (events 17 to 30), we also used data from the temporary stations of the SAPTEX array (see fig. 2.2). In table 2.III, *Seh* and *Sez* represent the 68% confidence estimates of the larger horizontal and the depth errors, respectively. Variable Δ_depth in the rightmost column shows the difference between the Hy-

Table 2.II. Location parameters of some deep earthquakes which occurred in peninsular Italy taken from the INGV seismic bulletin.

No.	Date	*M*	*Nph*	Origin time	Lat (N)	Long (E)	Depth	*Erh*	*Erz*	*Rms*	Region
1	04/08/1988	3.4	53	035710.5	39.220	14.603	517.5	5.9	12.0	0.5	Southern Tyrrhenian Sea
2	15/12/1989	2.5	25	143730.9	43.512	12.288	83.2	3.7	4.7	0.6	Northern Apennines
3	04/02/1990	2.2	17	010533.5	43.802	11.899	73.5	3.1	2.9	0.4	Northern Apennines
4	03/12/1990	2.5	23	181205.3	43.473	12.732	70.1	4.1	4.7	0.5	Northern Apennines
5	26/02/1991	4.5	80	072540.0	40.130	13.815	446.7	3.2	4.8	0.7	Southern Tyrrhenian Sea
6	03/09/1991	2.3	18	193710.7	40.589	15.481	41.5	3.6	4.5	0.5	Southern Apennines
7	09/12/1991	2.8	30	143955.3	44.470	10.558	96.4	3.7	9.2	0.7	Northern Apennines
8	18/01/1992	2.7	33	191413.2	39.851	16.159	83.2	2.3	2.8	0.4	Northern Calabria
9	24/04/1995	3.4	44	062318.3	39.204	16.316	64.0	2.4	4.5	0.6	Southern Tyrrhenian Sea
10	03/09/1995	2.7	28	134642.6	39.961	16.411	62.9	2.3	2.9	0.3	Northern Calabria
11	16/12/1995	3.1	39	060459.3	44.144	11.175	65.1	3.0	4.2	0.7	Northern Apennines
12	21/01/1996	3.4	62	121654.5	39.984	13.394	611.0	4.8	11.3	0.4	Southern Tyrrhenian Sea
13	21/12/1996	4.3	71	084535.3	39.878	13.188	681.4	4.6	10.1	0.4	Southern Tyrrhenian Sea
14	26/03/1998	4.7	56	162617.0	43.176	12.861	47.8	2.2	2.6	0.4	Northern Apennines
15	18/05/1998	5.1	73	171855.3	39.092	15.552	384.2	5.5	8.0	0.5	Southern Tyrrhenian Sea
16	21/07/1998	3.1	30	224708.5	40.485	15.031	338.6	4.4	5.1	0.2	Southern Apennines
17	11/07/2001	3.0	19	020625.3	40.217	13.739	459.5	8.4	10.6	0.3	Southern Tyrrhenian Sea
18	17/08/2001	4.1	47	031509.2	38.343	14.729	231.5	5.5	9.5	0.3	Aeolian Islands
19	18/10/2001	4.1	71	180830.9	38.523	15.092	236.1	3.3	5.0	0.4	Aeolian Islands
20	13/11/2001	2.4	16	132119.4	40.626	15.949	40.8	2.9	8.6	0.4	Southern Apennines
21	24/03/2002	2.8	23	001101.1	40.230	16.581	50.3	4.6	5.5	0.5	Basento Valley
22	12/05/2002	3.3	53	054655.9	40.036	15.463	363.0	4.3	5.6	0.3	Southern Tyrrhenian Sea
23	19/06/2002	3.1	23	152810.1	38.979	15.887	133.7	3.4	5.8	0.4	Southern Tyrrhenian Sea
24	30/10/2002	3.3	23	202920.1	38.154	17.322	65.0	5.1	10.6	0.4	Ionian Sea
25	01/12/2002	3.7	26	161802.0	38.719	14.842	296.4	2.2	3.2	0.4	Aeolian Islands
26	09/07/2003	3.2	42	102503.7	38.588	15.423	238.1	4.4	7.4	0.4	Southern Tyrrhenian Sea
27	14/11/2003	4.6	37	002158.5	40.339	14.568	378.1	3.4	2.8	0.5	Southern Tyrrhenian Sea
28	16/12/2003	3.2	33	011115.6	40.335	15.616	312.7	3.9	5.7	0.3	Southern Apennines
29	05/05/2004	5.3	34	133943.3	38.505	14.879	239.9	1.8	2.0	0.5	Aeolian Islands
30	19/09/2004	3.3	78	015840.8	40.350	12.864	516.5	7.4	9.5	0.8	Central Tyrrhenian Sea

Table 2.III. Hypoellipse relocation parameters for the deep earthquakes listed in table 2.II.

No.	Date	*Nph*	Origin Time	Lat (N)	Long (E)	Depth	*Seh*	*Sez*	*Rms*	Δ_depth (km)
1	04/08/1988	31	035721.91	39.156	14.695	433.5	2.1	9.3	0.47	−84.0
2	15/12/1989	16	143731.98	43.386	12.267	70.4	1.3	4.1	0.45	−12.8
3	04/02/1990	16	010533.74	43.752	11.884	71.8	3.6	3.5	0.45	−1.7
4	03/12/1990	14	181206.34	43.416	12.725	59.0	2.7	3.4	0.30	−11.1
5	26/02/1991	40	072543.18	40.019	13.943	442.4	1.5	5.6	0.38	−4.3
6	03/09/1991	18	193710.27	40.551	15.449	51.7	0.9	1.3	0.36	10.2
7	09/12/1991	17	143956.51	44.470	10.484	68.9	2.9	8.5	0.79	−27.5
8	18/01/1992	35	191413.33	39.819	16.175	84.0	0.7	1.1	0.51	0.8
9	24/04/1995	36	062317.57	39.182	16.324	71.0	1.7	2.5	0.45	7.0
10	03/09/1995	31	134642.18	39.965	16.423	68.9	1.0	1.7	0.27	6.0
11	16/12/1995	36	060459.09	44.097	11.159	70.0	0.6	1.1	0.86	4.9
12	21/01/1996	29	121707.92	39.936	13.286	518.5	2.2	9.3	0.44	−92.5
13	21/12/1996	44	084550.57	39.819	13.155	589.9	1.4	9.2	0.43	−91.5
14	26/03/1998	37	162617.08	43.124	12.806	45.2	0.5	0.7	0.49	−2.6
15	18/05/1998	34	171902.85	39.157	15.398	304.6	1.1	3.3	0.40	−79.6
16	21/07/1998	31	224711.27	40.557	15.082	315.5	2.0	3.9	0.18	−23.1
17	11/07/2001	16	020629.86	40.207	13.867	436.8	2.9	7.5	0.56	−22.7
18	17/08/2001	46	031511.30	38.392	14.687	214.9	0.6	1.6	0.49	−16.6
19	18/10/2001	51	180831.95	38.540	15.049	229.8	0.7	1.8	0.49	−6.3
20	13/11/2001	21	132119.75	40.560	15.949	42.8	0.7	1.3	0.19	2.0
21	24/03/2002	23	001059.96	40.279	16.684	61.2	0.8	0.7	0.74	10.9
22	12/05/2002	40	054659.52	40.041	15.371	335.8	1.0	2.7	0.27	−27.2
23	19/06/2002	44	152810.64	38.995	15.796	128.0	0.7	1.2	0.66	−5.7
24	30/10/2002	24	202920.39	38.195	17.288	69.0	1.7	2.6	0.48	4.0
25	01/12/2002	41	161803.44	38.734	14.795	284.5	0.8	1.1	0.35	−11.9
26	09/07/2003	44	102506.14	38.618	15.345	215.3	0.7	1.7	0.49	−22.8
27	14/11/2003	63	002156.63	40.375	14.579	405.1	0.9	2.9	0.41	27.0
28	16.12.2003	39	011119.63	40.311	15.557	277.3	0.7	1.2	0.39	−35.4
29	05/05/2004	41	133945.35	38.553	14.868	218.6	0.6	1.9	0.45	−21.3
30	19/09/2004	49	015844.65	40.251	12.808	468.1	2.2	5.1	0.32	−48.4

poellipse and the bulletin hypocentral depths. Most of the Δ_depth values are negative, especially for events deeper than 200 km as effect of the faster structure of the ak135 model with respect to the half space velocity adopted in the bulletin model. Indeed, the *P*-wave velocity predicted by the ak135 global model at 210 km depth is 8.30 km/s, increasing to about 10.90 km/s at 700 km in the lower mantle (Kennett *et al.*, 1995). The largest variation in the depth estimates (~−90 km) are observed for the two Southern Tyrrhenian deepest events, previously located below 600 km (see events 12 and 13 in tables 2.II and 2.III). It is interesting to note as the new locations fit better with the geometry of the high-velocity slabs depicted by the tomographic images in fig. 2.4c,d.

Finally, figs. 2.6 and 2.7 display the distribution with depth of the Northern Apennines and Southern Tyrrhenian subcrustal earthquakes, respectively. The 3D perspective images include the relocat-

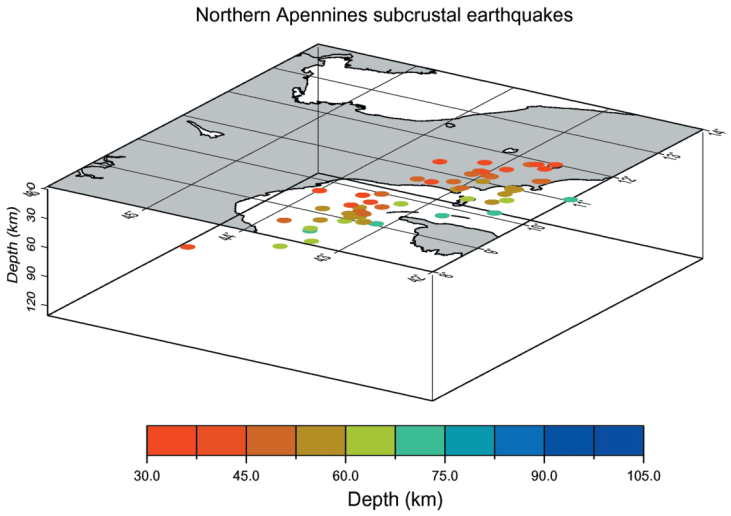

Fig. 2.6. Three-dimensional view from SW azimuth of the subcrustal earthquakes beneath the Northern Apennines region.

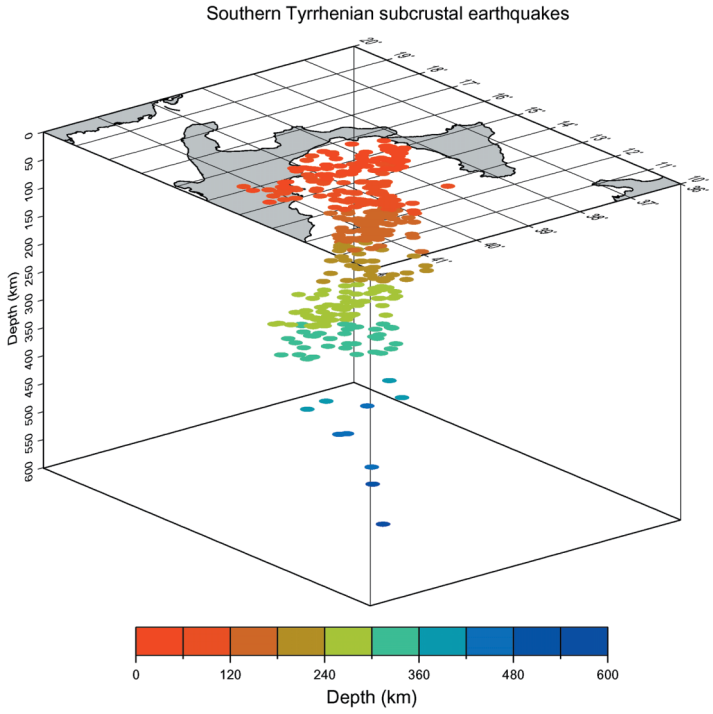

Fig. 2.7. Three-dimensional view from NW azimuth of the subcrustal earthquakes beneath the Southern Tyrrhenian area.

ed hypocentres given in table 2.III. For the Northern Apennines the view is from the SW, along cross-section AA′ (fig. 2.4a). The two seismogenic zones seen at the surface (fig. 2.5) extend in the uppermost mantle of the region without substantial differences in the concentration and/or in the maximum depths reached by the seismicity. The deepest events were relocated at slightly shallower depth, all around 70 km (table 2.III). This result indicates that the brittle, potentially seismogenic region of the descending lithosphere, is confined in the shallower portion of the ~300 km long slab reconstructed by tomography (fig. 2.4a).

For the Southern Tyrrhenian seismicity (fig. 2.7), the plot is drawn from the NW looking at the distribution along profile DD′ (fig. 2.4d). The pattern depicts a well developed Wadati-Benioff Zone characterized by a continuous, diffuse seismicity down to about 350 km depth, over a sparse deeper seismicity reaching maximum depths of about 600 km. At shallow depths (30÷70 km), the 3D view shows the subcrustal earthquakes located beneath the Ionian Sea, Calabria, and the Southern Apennines. The latter seismicity might not be related, however, to the seismogenic body associated with the Southern Tyrrhenian slab, but rather to the subduction of the continental Adriatic lithosphere.

2.5. Discussion

The tomographic models published in the past twenty years along with the deep seismicity studies carried out by numerous authors (Caputo *et al.*, 1970; Anderson and Jackson, 1987; Giardini and Velonà, 1991; Selvaggi and Amato, 1992; Amato *et al.*, 1993; Selvaggi and Chiarabba, 1995; Frepoli *et al.*, 1996), enhance the presence of remnants of past subduction beneath the entire Apenninic belt. In particular, as this study also makes clear, the morphology and the seismogenic characteristics of the inferred lithospheric sinkings delineate at least three basic types of the Apenninic subduction, dividing the range into different segments.

In the Northern Apennines, the upper mantle velocity structure is dominated by a continuous, steeply dipping slab that determines the present subsidence of the foredeep, a still active compressional front and widespread extension in the back-arc region (Frepoli and Amato, 1997). At present, the subduction process in this area is probably close to the end because of the exhaustion of the oceanic lithosphere available in front of the trench and of the amount of continental lithosphere already subducted into the mantle. The latter has been estimated as ~200 km in length during the last ~25 Myr (Gueguen *et al.*, 1998). The geometry of the high-velocity anomalies depicted by the tomographic images (fig. 2.4a), suggests that the present-day configuration was reached through progressive slab rollback, possibly determined by the older, deeper, oceanic lithosphere drawing from below. An alternative explanation of the near vertical dip of the slab is the proposed E-W mantle flow that could increase the plunge of the subducting lithosphere in west-dipping subduction zones like the Apennines (Doglioni, 1991). In any case, a clear discrepancy exists between the depth of the HVA (~300 km) and the seismogenic zone that appears confined in the uppermost mantle down to about 70 km. This observation may be related to a pronounced ductile behavior of the deepest portion of the subducting continental lithosphere, that is now aseismic (Carminati *et al.*, 2002).

Beneath the Central Apennines, a completely aseismic slab is recognized by our analysis from about 150 km down to the transition zone (fig. 2.4b). Broad, low-velocity anomalies are imaged beneath the chain and the pery-Tyrrhenian area down to ~300 km depth, suggesting asthenospheric upwelling in front of the subducting lithosphere. This hypothesis is corroborated by the studies on the propagation of *Pn* phases performed by Mele *et al.* (1996, 1998) who found strong evidence for a broad low-*Q*, low-velocity zone below the Moho. This high-attenuation region and the uppermost mantle slow structure reconstructed by the present teleseismic tomography join in a high-temperature mantle wedge that affects the thermal and rheological properties of the shallower, continental part of the Apenninic slab (Cimini and De Gori, 2001). A warmer, or less dense slab, could explain the absence of subcrustal earthquakes in this sector of Apenninic Chain.

The deep *P*-wave velocity structure in the Southern Apennines is dominated by a clear SW-ward dipping high-velocity body, probably related to the past oceanic subduction (fig. 2.4c). The slab portion between 200 and 400 km depth could represents the lithosphere subducted before the entrance of continental lithosphere in the Central-Southern Apennines, which most likely took place during the Messinian (6.5 Myr) as we can infer from paleomagnetic results (Speranza *et al.*, 1997). Unlike from the Central Apennines segment, some subcrustal earthquakes are observed in this sector within two distinct depth zones. The shallow seismicity is located beneath the chain but outside the HVA depicting the Southern Tyrrhenian subduction zone at such depths (Cimini 1999; Piromallo and Morelli, 2003). These events are also apparently detached from the main seismically active part of the slab (see fig. 2.7), suggesting they are part of a different piece of subducted lithosphere. The location of deep foci is strongly concident with the region of positive anomalies imaged by the tomographic reconstruction. The deepest events are located in the transition zone within the subhorizontal portion of the Tyrrhenian slab. The oceanic nature of this slab was proposed by Barberi *et al.* (1973) based on volcanological data, and by de Voogd *et al.* (1992) based on crustal thickness (~17 km in the Ionian area) and velocity profiles. The teleseismic image (fig. 2.4d) shows two main fast structures depicting a ~700 km long slab. This length is very close to the amount of eastward migration (~775 km) that affected the Apennines-Maghrebides subduction zone during the last 30-25 Myr (Gueguen *et al.*, 1998). The deeper, possibly detached part of the slab may hence represent the oldest portion (~20 Myr) of the subducted lithosphere. It lies subhorizontally in the transition zone beneath the Central Tyrrhenian Basin, suggesting a difficult penetration into a high-strength lower mantle. The lateral deflection seen in our tomographic reconstruction, as well as in previous investigations (Cimini, 1999; Lucente *et al.*, 1999; Piromallo and Morelli 2003), is corroborated by the fault-plane analysis of the deepest events, which shows subhorizontal dips for the *P*-axes (Frepoli *et al.*, 1996).

2.6. Conclusions

The combination of tomographic images with the distribution of well-located subcrustal earthquakes provides strong constraints for an improved definition of the upper mantle structure beneath peninsular Italy and surrounding seas. The resulting picture shows active and remnant subducted slabs in a general geodynamic context of oceanic-continental subduction. The along-strike complexity of the present-day Apenninic subduction, from the Northern Apennines to the Calabrian Arc, can be represented by at least three basic types of lithospheric sinking. The location of subcrustal events mostly coincides with the geometry of the slabs reconstructed by tomography, although some parts of the slabs appear to be aseismic. Future studies need to address this topic, investigating the rheological behavior and nature of the subducted lithosphere.

Acknowledgements

The authors would like to thank the two reviewers for their helpful comments and suggestions.

References

Aki, K., A. Christoffersson and E.S. Husebye (1977): Determination of the three-dimensional seismic structure of the lithosphere, *J. Geophys. Res*., **82**, 277-296.

Amato, A., B. Alessandrini, G.B. Cimini, A. Frepoli and G. Selvaggi (1993): Active and remnant subducted slabs beneath Italy: evidence from seismic tomography and seismicity, *Ann. Geofis.*, **XXXVI** (2), 201-214.

ANDERSON, H.J. and J. JACKSON (1987): The deep seismicity of the Tyrrhenian Sea, *Geophys. J. R. Astron. Soc*., **91**, 613-637.

BABUSKA, V. and J. PLOMEROVÁ (1990): Tomographic studies of the upper mantle beneath the Italian region, *Terra Nova*, **2**, 569-576.

BARBERI, F., P. GASPARINI, F. INNOCENTI and L. VILLARI, (1973): Volcanism of the Southern Tyrrhenian Sea and its geodynamic implications, *J. Geophys. Res*., **78**, 5221-5231.

CAPUTO, M., G.F. PANZA and D. POSTPISCHL (1970): Deep structure of the Mediterranean Basin, *J. Geophys. Res*., **75**, 4919-4923.

CARMINATI, E., F. GIARDINA and C. DOGLIONI (2002): Rheological control of subcrustal seismicity in the Apennines subduction (Italy), *Geophys. Res. Lett*., **29**, 1882.

CIMINI, G.B. (1999): *P*-wave deep velocity structure of the Southern Tyrrhenian Subduction Zone from non-linear teleseismic traveltime tomography, *Geophys. Res. Lett*., **26**, 3709-3712.

CIMINI, G.B. and A. AMATO (1993): *P*-wave teleseismic tomography: contribution to the delineation of the upper mantle structure of Italy, in *Recent Evolution and Seismicity of the Mediterranean Region*, edited by E. BOSCHI, E. MANTOVANI and A. MORELLI (Kluwer Academic Publishers, Dordrecht), 313-331.

CIMINI, G.B. and P. DE GORI (1997): Upper mantle velocity structure benath Italy from direct and secondary *P*-wave teleseismic tomography, *Ann. Geofis.*, **XL** (1), 175-194.

CIMINI, G.B. and P. DE GORI (2001): Non-linear *P*-wave tomography of subducted lithosphere beneath Central-Southern Apennines (Italy), *Geophys. Res. Lett*., **28**, 4387-4390.

CIMINI, G.B., P. DE GORI and A. FREPOLI (2006): Passive seismology in Southern Italy: the SAPTEX array, *Ann. Geophysics*, **49** (2/3) (in press).

DERCOURT, J., L.P. ZONENSHAIN, L.-E. RICOU, V.G. KAZMIN, X. LE PICHON, A.L. KNIPPERH, C. GRANDJACQUET, I.M. SBORTSHIKOV, J. GEYSSANT, C. LEPVRIER, D.H. PECHERSKY, J. BOULIN, J.-C. SIBUET, L.A. SAVOSTIN, O. SOROKHTIN, M. WESTPHAL, M.L. BAZHENOV, J.P. LAUER and B. BIJU-DUVAL (1986): Geological evolution of the tethys belt from the atlantic to the pamirs since the LIAS, *Tectonophysics*, **123** (1-4), 241-315.

DE VOOGD, B., C. TRUFFERT, N. CHAMOT-ROOKE, P. HUCHON, S. LALLEMANT and X. LE PICHON (1992): Two-ships deep seismic soundings in the basin of the Eastern Mediterranean Sea (Pasiphae cruise), *Geophys. J. Int*., **109**, 536-552.

DEWEY, J.F., M.L. HELMAN, E. TURCO, D.W.H. HUTTON and S.P. KNOTT (1989): Kinematics of the Western Mediterranean, in *Alpine Tectonics*, edited by M.P. COWARD, D. DIETRICH and R.G. PARK, *Geol. Soc. London, Spec. Publ.*, **45**, 265-283.

DI STEFANO, R., C. CHIARABBA, F. LUCENTE and A. AMATO (1999): Crustal and uppermost mantle structure in Italy from the inversion of *P*-wave arrival times: geodynamics implications, *Geophys. J. Int.,* **139**, 483-498.

DOGLIONI, C. (1991): A proposal for the kinematic modelling of W dipping subductions – Possible applications to the Tyrrhenian-Apennines system, *Terra Nova*, **3**, 423-434.

FACCENNA, C., P. DAVY, J.B. BRUN, R. FUNICIELLO, D. GIARDINI, M. MATTEI and T. NALPAS (1996): The dynamics of back-arc extension: an experimental approach to the opening of the Tyrrhenian Sea, *Geophys. J. Int*., **126**, 781-795.

FREPOLI, A. and A. AMATO (1997): Contemporaneous extension and compression in the Northern Apennines from earthquake fault plane solutions, *Geophys. J. Int*., **125**, 879-891.

FREPOLI, A., G. SELVAGGI, C. CHIARABBA and A. AMATO (1996): State of stress in the Southern Tyrrhenian subduction zone from fault-plane solutions, *Geophys. J. Int*., **125**, 879-891.

GIARDINI, D. and M. VELONÀ (1991): The deep seismicity of the Tyrrhenian Sea, *Terra Nova*, **3**, 57-64.

GUEGUEN, E., C. DOGLIONI and M. FERNANDEZ (1998): On the post-25 Myr geodynamic evolution of the Western Mediterranean, *Tectonophysics*, **298**, 259-269.

HIRAHARA, K. and A. HASEMI (1993): Tomography of subduction zones using local and regional earthquakes and teleseisms, in *Seismic Tomography: Theory and Practice*, edited by H.M. IYER and K. HIRAHARA (Chapman & Hall, London), 519-562

KENNETT, B.L.N., E.R. ENGDHAL and R. BULAND (1995): Constraints on seismic velocities in the Earth from traveltimes, *Geophys. J. Int*., **126**, 555-578.

LAHR, J.C. (1999): Hypoellipse: a computer program for determining local earthquake hypocentral parameters, magnitude, and first-motion pattern, *U.S. Geol. Surv. Open-File Rep. 99-23*.

LAY, T. (1994): *Seismological Structure of Slabs* (Academic Press, San Diego), pp. 185.

LUCENTE, F.P., C. CHIARABBA, G.B. CIMINI and D. GIARDINI (1999): Tomographic constraints on the geodynamic evolution of the Italian region, *J. Geophys. Res*., **104**, 20,307-20,327.

MALINVERNO, A. and W.B.F. RYAN (1986): Extension in the Tyrrhenian Sea and shorthening in the Apennines as result of arc migration driven by the sinking of the lithosphere, *Tectonics*, **5**, 227-245.

MELE, G., A. ROVELLI, D. SEBER and M. BARAZANGI (1996): Lateral variations of *Pn* propagation in Italy: evidence for a high-attenuation zone beneath the Apennines, *Geophys. Res. Lett.,* **23**, 709-712.

MELE, G., A. ROVELLI, D. SEBER, M.T. HEARN and M. BARAZANGI (1998): Compressional velocity structure and anisotropy in the uppermost mantle beneath Italy and surrounding regions, *J. Geophys. Res*., **103**, 12529-12543.

PATACCA, E., R. SARTORI and P. SCANDONE (1990): Tyrrhenian Basin and Apenninic arcs: kinematic relations since Late Tortonian times, *Mem. Soc. Geol. It*., **45**, 425-451.

PIROMALLO, C. and A. MORELLI (1997): Imaging the Mediterranean upper mantle by *P*-wave travel time tomography, *Ann. Geofis.*, **XL** (4), 963-979.

PIROMALLO, C. and A. MORELLI (2003): *P*-wave tomography of the mantle under the Alpine-Mediterranean area, *J. Geophys. Res*., **108** (B2), 2065, doi: 10.1029/2002JB001757.

SCARPA, R. (1982): Travel-time residuals and three-dimensional velocity structure of Italy, *Pure Appl. Geophys.*, **120**, 583-606.

SELVAGGI, G. and A. AMATO (1992): Intermediate-depth earthquake in Northern Apennines (Italy): evidence for a still active subduction?, *Geophys. Res. Lett.,* **19**, 2127-2130.

SELVAGGI, G. and C. CHIARABBA (1995): Seismicity and *P*-wave velocity image of the Southern Tyrrhenian subduction zone, *Geophys. J. Int.,* **121,** 818-826.

SPAKMAN, W., S. VAN DER LEE and R.D. VAN DER HILST (1993): Travel-time tomography of the European-Mediterranean mantle down to 1400 km, *Phys. Earth Planet. Inter*., **79**, 3-74.

SPERANZA, F., L. SAGNOTTI and M. MATTEI (1997): Tectonics of the Umbria-Marche-Romagna Arc (Central-Northern Apennines, Italy): new paleomagnetic constraints*, J. Geophys. Res*., **102**, 3153-3166.

WILSON, M. and G. BIANCHINI (1999): Tertiary-Quaternary magmatism within the Mediterranean and surrounding regions, in *The Mediterranean Basins: Tertiary Extension within the Alpine Orogen*, edited by B. DURAND, L. JOLIVET, F. HORVATH and M. SERRANE, *Geol. Soc. London, Spec. Publ.*, **156**, 141-168.